Mathematics Today Vol.34(A) (April 2018 – Special Issue) 120-133
ISSN 0976-3228, e-ISSN 2455-9601

# Thermal Diffusion and Diffusion Thermo Effects on Two Dimensional MHD Casson Fluid Flow with Thermal Radiation In Porous Medium

Dr. Hari R. Kataria[1] and Mr. Rakesh R Darji[2]

[1]Department of Mathematics, Faculty of Science,
The M. S. University of Baroda, Vadodara, India
[1]hrkrmaths@yahoo.com

[2]Applied Science & Humanities Department,
SardarVallabhbhai Patel Institute of Technology, Vasad, India
[2]darjirakesh12@gmail.com

**Corresponding author:** Rakesh R Darji[2]

## Abstract

In this study, effects of thermal diffusion, diffusion thermo and thermal radiation effects on two dimensional MHD Casson fluid flows over a stretched surface in porous medium is studied. The governing dimensionless system of ordinary differential equations are solved using Homotopy analysis method which is obtained by reducing original system of partial differential equations using suitable change of variables. Effects of different prevailing parameters: Radiation parameter, thermal diffusion parameter, diffusion thermo parameter, Magnetic parameter and Casson fluid parameter on Heat and mass transfer of two dimensional MHD flow are discussed and represented through graph. Expression for Skin friction, Nusselt number and Sherwood number are also derived. From graphical presentation, we observed that magnetic field tends to reduced motion of the fluid whereas thermal radiation and permeability of porous medium have reverse effects on it.

**Keywords**: HAM; MHD; Casson fluid; Heat transfer; Mass transfer

**AMS Mathematics Subject Classification**: 76W05, 76W99

**Nomenclature**

| | |
|---|---|
| $T$ | Temperature |
| $T_w$ | Temperature |
| $u, v$ | Velocity components along $x, y$ axes, respectively |
| $B_0$ | External uniform magnetic field |
| $C_p$ | Specific heat at constant pressure |
| g | Acceleration due to gravity |
| $k_1$ | Thermal conductivity |
| $k$ | Permeability of the fluid |
| $De$ | Mass diffusivity |
| $Sc$ | Schmidt number |

$Sr$ Soret Number

M Magnetic parameter (Ratio of Lorentz force to viscous force)

$Pr$ Prandtl number (ratio of momentum diffusivity to thermal diffusivity)

Greek symbols

$\alpha$ Thermal diffusivity

$\rho$ Density

$\sigma$ Electrical conductivity (S/m)

$\theta$ Dimensionless temperature ($\theta = \frac{T-T_0}{T_w-T_0}$)

$\mu$ Dynamic viscosity

$\varphi$ Porosity

$\kappa$ Permeability (dimensionless)

$\gamma$ Casson fluid parameter

$\nu$ Kinematic viscosity

$\eta$ Dimensionless variable

Subscripts

$f$ Fluid phase

$s$ Solid phase

**1. Introduction:**

The analysis of non-Newtonian fluid flows generated by a stretching sheet has a great role in several manufacturing processes such as extrusion of molten polymers through a slit die for the production of plastic sheet, processing of food stuffs, paper production, wire and fiber coating to mention few among others. The quality of final product in such processes greatly depends upon the rate of cooling in the heat transfer process. The MHD consideration is one of the important parameters by which cooling rate can be controlled and the product of desired quality can be achieved. Crane [1] was the first among the others to provide the closed form solution for steady and two-dimensional incompressible boundary layer flow of viscous fluid generated by a stretching surface. This flow problem has been extended under diverse physical aspects in the form of series of papers by the different researchers in the field. The aspect of the current research is to examine the effects of thermal diffusion, diffusion thermo and thermal radiation effects on two dimensional MHD Casson fluid flows over a stretched surface in porous medium. Yao, Chen [2] discussed the series solution with stretching boundary. Sheikholeslami and Bhatti [3] solved by active method for nanofluid heat transfer problem. Hayat et. al [4, 5] studied stretching flow with heat flux. Kataria and Patel [6-10] discussed MHD flow for different fluid with different situation. Hayat et. al[11] also studied peristalsis of Eyring-Powell magneto nanomaterial considering Darcy-Forchheimer relation. Kataria and Mittal [12, 14] analyzed velocity, mass and temperature of nanofluid flow in a porous medium. Kataria and Mittal [15] investigated effect of radiation on Casson nanofluid

flow. Hayat et. al[16-19] discussed the problem for different fluid in presence of different conditions. Sheikholeslami et. al[20-23] studied different model like two phase model, Buongiorno model. Koo and Kleinstreuer [24, 25] analyzed laminar fluid flow and viscous dissipation.

The aim of this paper is to study the control of heat and mass transfer through thermal diffusion and diffusion thermo in presence of thermal radiation in two dimensional problems.

**2. Problem statement**

Let us considered the steady MHD two dimensional Casson fluid flow over a heated stretched surface at $y = 0$ as shown in Figure 1. A Cartesian coordinate system $(x, y)$ are chosen such that $x$- axis is parallel to stretched surface whereas $y$ - axis as normal to it. A constant magnetic field $B_0$ is applied in the transverse direction to the surface. Due to small magnetic Reynold number induced magnetic field are negligible. Also fluid is incompressible and flow in two dimensional. We consider this problem due to the effects of thermal diffusion and diffusion-thermo effects on the MHD flow.

The constitutive equation for the Casson fluid can be written as

$$\tau_{ij} = \begin{cases} 2\left(\mu B + \frac{Py}{\sqrt{2\pi}}\right) e_{ij} & \pi > \pi_c \\ 2\left(\mu B + \frac{Py}{\sqrt{2\pi_c}}\right) e_{ij} & \pi < \pi_c \end{cases} \tag{1}$$

Where $\pi = e_{ij}e_{ij}$ and $e_{ij}$ is the $(i, j)^{th}$ component of the deformation rate, $\pi$ is the product of the component of deformation rate with itself, $\pi_c$ is a critical value of this product based on the non- Newtonian model, $\mu B$ is plastic dynamic viscosity of the non-Newtonian fluid and $P_y$ is yield stress of fluid.

$$P_y = \frac{\mu B\sqrt{2\pi}}{\gamma} \tag{2}$$

From the definition of viscosity given by Batchelor [26], ratio of sheer stress $\tau^*$ to viscosity $\mu$ is constant in case of Newtonian.

$$\tau^* = \mu\frac{\partial u}{\partial y} \tag{3}$$

Some fluids require a gradually increasing shear stress to maintain a constant strain rate, In the case of Casson fluid (Non Newtonian) flow where $\pi > \pi_c$

$$\mu = \mu B + \frac{P_y}{\sqrt{2\pi}} \tag{4}$$

Substituting equation (2) in equation (4), the Kinematics viscosity can be expressed as

$$\nu = \frac{\mu B\left(1+\frac{1}{\gamma}\right)}{\rho} \tag{5}$$

The resulting boundary layer equations in MHD flow under consideration are

$$\frac{\partial u}{\partial x}+\frac{\partial v}{\partial y}=0 \tag{6}$$

$$\left(u\frac{\partial u}{\partial x}+v\frac{\partial u}{\partial y}\right)=\nu\left(1+\frac{1}{\gamma}\right)\frac{\partial^2 u}{\partial y^2}-\sigma B_0^2 u-\frac{\mu\emptyset}{k'}u \tag{7}$$

$$\left(u\frac{\partial T}{\partial x}+v\frac{\partial T}{\partial y}\right)=\frac{k_4}{\rho c_p}\frac{\partial^2 T}{\partial y^2}-\frac{1}{\rho c_p}\frac{\partial q_r}{\partial y}+\frac{D_e k_T}{C_s C_p}\frac{\partial^2 C}{\partial y^2} \tag{8}$$

$$\left(u\frac{\partial C}{\partial x}+v\frac{\partial C}{\partial y}\right)=D_e\frac{\partial^2 C}{\partial y^2}+\frac{D_e k_T}{T_m}\frac{\partial^2 T}{\partial y^2} \tag{9}$$

$$u=ax;\ v=0;\ T=T_w;C=C_w\ at\ y=0 \tag{10}$$

$$u\to 0,T\to T_\infty,\ \ C\to C_\infty;\ as\ \ y\to\infty\ and\ t\geq 0 \tag{11}$$

$$\eta=y\sqrt{\frac{a}{\nu}},\ u=axf'(\eta),v=-\sqrt{a\nu}f(\eta),\ \theta(\eta)=\frac{T-T_\infty}{T_w-T_\infty},C(\eta)=\frac{C-C_\infty}{C_w-C_\infty} \tag{12}$$

The local radiant for the case of an optically thin gray gas is expressed by Rosseland approximation [27]

$$\frac{\partial q_r}{\partial y}=-4a^*\sigma^*(T'^4_\infty-T'^4)$$

where $\sigma^*$ and $a^*$ are Stefan Boltzmann constant and absorption coefficient respectively.

Using the Taylor's series, expand $T'^4$about $T'_\infty$ and neglecting higher order terms,

$$T'^4\cong 4T'^3_\infty T'-3T'^4_\infty$$

Therefore, the governing momentum and energy equations for this problem are given in dimensionless form by:

$$\left(1+\frac{1}{\gamma}\right)f'''+ff''-f'^2-\left(M^2+\frac{1}{k}\right)f'=0 \tag{13}$$

$$\left(\frac{1+Nr}{Pr}\right)\theta''+f\theta'-\theta f'+Du\,C''=0 \tag{14}$$

$$C''+\Pr Le\,fC'-Pr\ Le\ Cf'+SrLe\theta''=0 \tag{15}$$

$$f(0)=0,f'(0)=1\,,f'(\infty)=0\,,$$
$$\theta(0)=1,\theta(\infty)=0\,,$$
$$C(0)=1,C(\infty)=0\,, \tag{16}$$

where

$$M^2=\frac{\sigma {B_0}^2}{\rho {U_0}^2}t_0,\ \frac{1}{k}=\frac{\nu\phi^2}{k'{U_0}^2},\ \gamma=\frac{\mu_B\sqrt{2\pi_c}}{P_y},\ Le=\frac{\nu}{D_e},Nr=-\frac{16\,a^*\sigma^*\nu^2{T'}_\infty^{\,3}}{k_4{U_0}^2},\ Re=\frac{aL^2}{v_f},Pr=\frac{\rho c_p}{k_4}\,,Du=$$
$$\frac{D_e k_T}{C_s C_p}\frac{C_w-C_\infty}{(T_w-T_\infty)\vartheta}\,,Sr=\frac{D_e k_T}{T_m\vartheta}\frac{T_w-T_\infty}{(C_w-C_\infty)} \tag{17}$$

Dimensionless expression of the local skin-friction coefficient, the local Nusselt number and the local Sherwood number are

$$Re^{1/2}Cf = \left(1 + {}^{1}/_{\gamma}\right)f''(0), \tag{18}$$

$$Nu(Re)^{-1/2} = -\theta'(0), \tag{19}$$

$$Sh(Re)^{-1/2} = -C'(0). \tag{20}$$

**3. Solution by Homotopy Analysis Method**

Homotopy analysis method is a fundamental concept of topology. Equations (13) – (15) are coupled non-linear ordinary differential equations and exact solutions are not possible. To solve these equations together with the boundary conditions (16), the modified homotopy analysis method (HAM) suggested by Liao [28] is employed.

Initial guess is given by:

$$f_0(\eta) = 1 - e^{-\eta};\ \theta_0(\eta) = e^{-\eta};\ C_0(\eta) = e^{-\eta}; \tag{21}$$

with auxiliary linear operators:

$$L_f = \frac{\partial^3 f}{\partial \eta^3} - \frac{\partial f}{\partial \eta}\ ,\ L_\theta = \frac{\partial^2 \theta}{\partial \eta^2}\ ,\ \ L_C = \frac{\partial^2 C}{\partial \eta^2} \tag{22}$$

Satisfying

$$L_f(C_1 + C_2 e^{\eta} + C_3 e^{-\eta}) = 0,\ L_\theta(C_4 + C_5\eta) = 0,\ \ L_C(C_6 + C_7\eta) = 0. \tag{23}$$

where $c_1,\ c_2, \ldots., c_7$ are the arbitrary constants.

The zero[th] order deformation problems are constructed as follows:

$$(1-p)L_f\left[\hat{f}(\eta;\ p) - f_0(\eta)\right] = p\hbar_f N_f\left[\hat{f}(\eta;\ p), \hat{\theta}(\eta;\ p), \hat{C}(\eta;\ p)\right], \tag{24}$$

$$(1-p)L_\theta\left[\hat{\theta}(\eta;\ p) - \theta_0(\eta)\right] = p\hbar_\theta N_\theta\left[\hat{f}(\eta;\ p), \hat{\theta}(\eta;\ p), \hat{C}(\eta;\ p)\right], \tag{25}$$

$$(1-p)L_C\left[\hat{C}(\eta;\ p) - C_0(\eta)\right] = p\hbar_C N_C\left[\hat{f}(\eta;\ p), \hat{\theta}(\eta;\ p), \hat{C}(\eta;\ p)\right], \tag{26}$$

Subject to the boundary conditions:

$$\hat{f}(0;\ p) = 0, \quad \hat{f}'(0;\ p) = 1; \tag{27}$$

$$\hat{f}'(\infty;\ p) = 0; \tag{28}$$

$$\hat{\theta}(0;\ p) = 1, \quad \hat{\theta}(\infty;\ p) = 0; \tag{29}$$

$$\hat{C}(0;\ p) = 1, \quad \hat{C}(\infty;\ p) = 0. \tag{30}$$

The nonlinear operator are defined as

$$N_f\left[\hat{f}(\eta;\ p), \hat{\theta}(\eta;\ p), \hat{C}(\eta;\ p)\right] = \left(1 + \frac{1}{\gamma}\right)\frac{\partial^3 \hat{f}}{\partial \eta^3} + \hat{f}\frac{\partial^2 \hat{f}}{\partial \eta^2} - \left(\frac{\partial \hat{f}}{\partial \eta}\right)^2 - \left(M^2 + \frac{1}{k}\right)\frac{\partial \hat{f}}{\partial \eta}\ , \tag{31}$$

$$N_\theta\left[\hat{f}(\eta;\ p), \hat{\theta}(\eta;\ p), \hat{C}(\eta;\ p)\right] = \left(\frac{1+Nr}{Pr}\right)\frac{\partial^2 \hat{\theta}}{\partial \eta^2} + \hat{f}\frac{\partial \hat{\theta}}{\partial \eta} - \hat{\theta}\frac{\partial \hat{f}}{\partial \eta} + Du\frac{\partial^2 \hat{C}}{\partial \eta^2}, \tag{32}$$

$$N_C\left[\hat{f}(\eta;\ p), \hat{\theta}(\eta;\ p), \hat{C}(\eta;\ p)\right] = \frac{\partial^2 \hat{C}}{\partial \eta^2} + \mathrm{Pr}\,Le\,\hat{f}\frac{\partial \hat{C}}{\partial \eta} - \mathrm{Pr}\,Le\,\hat{C}\frac{\partial \hat{f}}{\partial \eta} + SrLe\frac{\partial^2 \hat{\theta}}{\partial \eta^2} \tag{33}$$

Where $\hat{f}(\eta;\ p), \hat{\theta}(\eta;\ p)$ and $\hat{C}(\eta;\ p)$ are unknown functions with respect to $\eta$ and $p$. $\hbar_f$, $\hbar_\theta$ and $\hbar_C$ are the non-zero auxiliary parameters and $N_f$, $N_\theta$ and $N_C$ are the nonlinear operators.

Also $p \in (0,\ 1)$ is an embedding parameter. For $p = 0$ and $p = 1$ we have

$$\hat{f}(\eta; 0) = f_0(\eta), \hat{f}(\eta; 1) = f(\eta), \tag{34}$$

$$\hat{\theta}(\eta; 0) = \theta_0(\eta), \hat{\theta}(\eta; 1) = \theta(\eta), \tag{35}$$

$$\hat{C}(\eta; 0) = C_0(\eta), \hat{C}(\eta; 1) = C(\eta), \tag{36}$$

In other words, when variation of $p$ is taken from 0 to 1 then $\hat{f}(\eta;\ p)$, $\hat{\theta}(\eta;\ p)$ and $\hat{C}(\eta;\ p)$ vary from $f_0(\eta), \theta_0(\eta)$, and $C_0(\eta)$ to $f(\eta), \theta(\eta),$ and $C(\eta)$. Taylor's series expansion of these functions yields the following:

$$\hat{f}(\eta;\ p) = f_0(\eta) + \sum_{m=1}^{\infty} f_m(\eta) p^m, \tag{37}$$

$$\hat{\theta}(\eta;\ p) = \theta_0(\eta) + \sum_{m=1}^{\infty} \theta_m(\eta) p^m, \tag{38}$$

$$\hat{C}(\eta;\ p) = C_0(\eta) + \sum_{m=1}^{\infty} C_m(\eta) p^m, \tag{39}$$

Where

$$f_m(\eta) = \frac{1}{m!}\left[\frac{\partial^m f(\eta; p)}{\partial p^m}\right]_{p=0}, \tag{40}$$

$$\theta_m(\eta) = \frac{1}{m!}\left[\frac{\partial^m \theta(\eta; p)}{\partial p^m}\right]_{p=0}, \tag{41}$$

$$C_m(\eta) = \frac{1}{m!}\left[\frac{\partial^m C(\eta; p)}{\partial p^m}\right]_{p=0}, \tag{42}$$

It should be noted that the convergence in the above series strongly depends upon $\hbar_f, \hbar_\theta$ and $\hbar_C$. Assuming that these nonzero auxiliary parameters are chosen so that Eqs.(37)-(39) converges at $p = 1$, Hence one can obtain the following:

$$f(\eta) = f_0(\eta) + \sum_{m=1}^{\infty} f_m(\eta), \tag{43}$$

$$\theta(\eta) = \theta_0(\eta) + \sum_{m=1}^{\infty} \theta_m(\eta), \tag{44}$$

$$C(\eta) = C_0(\eta) + \sum_{m=1}^{\infty} C_m(\eta), \tag{45}$$

Differentiating the zero[th] order deformation (24) – (26) and (27) – (30) $m$ times with respect to $p$ and substituting $p = 0$ , and finally dividing by ! , we obtain the $m^{th}$ order deformation ($m \geq 1$).

$$L_f[f_m(\eta) - \chi_m f_{m-1}(\eta)] = \hbar_f R_{f,m}(\eta), \tag{46}$$

$$L_\theta[\theta_m(\eta) - \chi_m \theta_{m-1}(\eta)] = \hbar_\theta R_{\theta,m}(\eta), \tag{47}$$

$$L_C[C_m(\eta) - \chi_m C_{m-1}(\eta)] = \hbar_C R_{C,m}(\eta), \tag{48}$$

Subject to the boundary conditions

$$f_m(0) = 0, \tag{49}$$

$$f_m'(0) = f_m'(\infty) = 0, \tag{50}$$

$$\theta_m(0) = \theta_m(\infty) = 0, \tag{51}$$

$$C_m(0) = C_m(\infty) = 0, \tag{52}$$

with

$$R_{f,m}(\eta) = \left(1 + \frac{1}{\gamma}\right) f'''_{m-1} + \sum_{j=0}^{m-1} f_j f''_{m-1-j} - \sum_{j=0}^{m-1} f_j'^2 - \left(M^2 + \frac{1}{k}\right) f'_{m-1} \tag{53}$$

$$R_{\theta,m}(\eta) = \left(\frac{1+Nr}{Pr}\right) \theta''_{m-1} + \sum_{j=0}^{m-1} f_j \theta'_{m-1-j} - \sum_{j=0}^{m-1} f'_j \theta_{m-1-j} + D_f C''_{m-1} \tag{54}$$

$$R_{C,m}(\eta) = C''_{m-1} + \Pr Le \sum_{j=0}^{m-1} f_j C'_{m-1-j} - \sum_{j=0}^{m-1} f'_j C_{m-1-j} + SrLe\theta''_{m-1} \tag{55}$$

$$\text{with } \chi_m = \begin{cases} 0, & m \le 1 \\ 1, & m \ge 1 \end{cases}, \tag{56}$$

Solving the corresponding $m^{th}$-order deformation equations,

$$f_m(\eta) = f_m^*(\eta) + C_1 + C_2 e^{\eta} + C_3 e^{-\eta} \tag{57}$$

$$\theta_m(\eta) = \theta_m^*(\eta) + C_4 + C_5 \eta \tag{58}$$

$$C_m(\eta) = C_m^*(\eta) + C_6 + C_7 \eta \tag{59}$$

Here $f_m^*, \theta_m^* \; and \; C_m^*$ are given by are particular solutions of the corresponding $m^{th}$-order equations and the constants $C_i (\, i = 1,2, \ldots ,7)$ are to be determined by the boundary conditions.

**4. Results and Discussion:**

To understanding the physics of the problem, the solutions are obtained using codes in Mathematica. The solution obtained by mathematica having long series expression. It is difficult to write all series expression in the manuscript. Obtained results are explained with the help of graphs. Parametric study is performed for Soret number $Sr$, Radiation parameter $Nr$, Magnetic parameter $M$ and Permeability parameter $k$.

Figure 2 show effects of magnetic field $M$ on velocity profiles. It is seen that, velocity in $y$- direction is decrease with increase in $M$. Physically, when magnetic field can induce current in the conductive fluid and create Lorentz force on the fluid in the boundary layer, which slow down the velocity of the fluid. Therefore, the magnetic field acts like a drag force.

Figure 3 shows the effect on velocity profiles for different values of Casson parameter $\gamma$, when the other parameters are fixed. It is observed that velocity of the fluid decreases with increasing values Casson parameter $\gamma$. An increase in Casson parameter makes the velocity boundary layer thickness shorter and hence motion of the fluid is decelerated.

Figures 4 show effects of Permeability parameter $k$ on velocity profiles. It is seen that velocity increases with increasing $k$. This is true due to the effects of drag force. Physically, If we increase permeability of porous medium $k$, hole of porosity will be increase which is improve motion in $y$-direction.

Figures 5 show effects of thermal radiation parameter $Nr$ on temperature profiles. Physically, due to increasing thermal radiation parameter $Nr$, heat is generated in fluid flow, which leads to improvement in heat transfer process.

Figure 6-9 show effects of soret and dufour effect on temperature and concentration profiles. It is seen that Dufour number tends to improved heat transfer process and reduced mass transfer process, while soret number is opposite effects compared to Dufour number on temperature and concentration profiles.

Figure 10 exhibits the concentration profiles for different values of Schmidt number $Sc$. It is observed that mass transfer process decreases with increase in $Sc$.

**5. Conclusion:**

- Velocity profile declines with escalation in Magnetic parameter $M$ and Casson parameter $\gamma$
- Velocity increases with permeability parameter $k$
- Temperature increase with increase in radiation parameter $Nr$ and Dufour effect $Du$.
- Temperature tends to decrease with rising Soret effect $Sr$.
- Concentration profile increase with increase in Soret effect $Sr$ and decrease with increase in Schdimt number $Sc$ and Dufour effect $Du$.

**References:**

[1] Crane, L. J., (1970): Flow past a stretching plate, Z. Angew. Math. Phys., 21, 645-647.

[2] Yao, B., Chen, J., (2009): Series solution to the Falkner-Skan equation with stretching boundary, Applied Math. Comput., 208, 156-164.

[3] Sheikholeslami, M., Bhatti, M. M., (2017): Active method for nanofluid heat transfer enhancement by means of EHD, Int. J. Heat Mass Transfer, 109, 115–122.

[4] Hayat, T., Khan, M. I., Farooq, M., Alsaedi, A., Khan, M. I., (2017): Thermally stratified stretching flow with Cattaneo–Christov heat flux, Int. J. Heat Mass Transfer, 106, 289-294.

[5] Hayat, T., Qayyum, S., Alsaedi, A., Ahmad, B., (2017): Magnetohydrodynamic (MHD) nonlinear convective flow of Walters-B nanofluid over a nonlinear stretching sheet with variable thickness, Int. J. Heat Mass Transfer, 110, 506-514.

[6] Kataria, H. R., Patel, H. R., (2016): Heat and Mass Transfer in MHD Second Grade Fluid Flow with Ramped Wall Temperature through Porous Medium, Mathematics Today, 32, 67-83.

[7] Kataria, H. R., Patel, H. R., (2016): Radiation and chemical reaction effects on MHD Casson fluid flow past an oscillating vertical plate embedded in porous medium, Alex. Eng. J., 55, 583-595.

[8] Kataria, H. R., Patel, H. R., (2016): Soret and heat generation effects on MHD Casson fluid flow past an oscillating vertical plate embedded through porous medium, Alex. Eng. J., 55, 2125–2137.

[9] Kataria, H. R., Patel, H. R., (2016): Effect of thermo-diffusion and parabolic motion on MHD Second grade fluid flow with ramped wall temperature and ramped surface concentration, Alex. Eng. J., https://doi.org/10.1016/j.aej.2016.11.014.

[10] Kataria, H. R., Patel, H. R., Singh, R., (2017): Effect of magnetic field on unsteady natural convective flow of a micropolar fluid between two vertical walls, Ain Shams Engineering J. 8, 87–102.

[11] Hayat, T., Farooq, S., Ahmad, B., Alsaedi, A., (2017): Peristalsis of Eyring-Powell magneto nanomaterial considering Darcy-Forchheimer relation, Int. J. Heat Mass Transfer, 115, 694-702.

[12] Kataria, H. R., Mittal, A. S., (2017): Velocity, mass and temperature analysis of gravity-driven convection nanofluid flow past an oscillating vertical plate in presence of magnetic field in a porous medium, Applied Thermal Engineering, 110, 864-874

[13] Sheikholeslami, M., Zeeshan, A., (2017): Mesoscopic simulation of CuO-H2O nanofluid in a porous enclosure with elliptic heat source, Int. J. Hydrogen Energy,42, 15393-15402

[14] Kataria, H. R., Mittal, A. S., (2015): Mathematical model for velocity and temperature of gravity-driven convective optically thick nanofluid flow past an oscillating vertical plate in presence of magnetic field and radiation., J. Nigerian Math. Soc., 34, 303–317.

[15] Kataria, H. R., Mittal, A. S., (2017): Analysis of Casson Nanofluid Flow in Presence of Magnetic Field and Radiation, Mathematics Today, 33(1), 99 - 120.

[16] Hayat, T., Waqas, M., Khan, M. I., Alsaedi, A., Shehzad, S.A., (2017): Magnetohydrodynamic flow of burgers fluid with heat source and power law heat flux, Chin. J. Phys., 55, 318-330.

[17] Hayat, T., Nazar, H., Imtiaz, M., Alsaedi, A., Ayub, M., (2017): Axisymmetric squeezing flow of third grade fluid in presence of convective conditions, Chin. J. Phys., 55, 738-754.

[18] Waqas, M., Khan, M. I., Hayat, T., Alsaedi, A., Khan, M. I., (2017): On Cattaneo–Christov double diffusion impact for temperature-dependent conductivity of Powell–Eyring liquid, Chin. J. Phys., 55, 729-737.

[19] Hayat, T., Zubair, M., Waqas, M., Alsaedi, A., Ayub, M., (2017): Application of non-Fourier heat flux theory in thermally stratified flow of second grade liquid with variable properties, Chin. J. Phys., 55, 230-241.

[20] Sheikholeslami, M., Rokni, H. B., (2017): Influence of melting surface on MHD nanofluid flow by means of two phase model, Chin. J. Phys., 55, 1352-1360.

[21] Sheikholeslami, M., Rokni, H. B., (2017): Effect of melting heat transfer on nanofluid flow in existence of magnetic field considering Buongiorno Model, Chin. J. Phys., 55, 1115-1126.

[22] Sheikholeslami, M., Shehzad, S.A., (2017): Thermal radiation of ferrofluid in existence of Lorentz forces considering variable viscosity, Int. J. Heat Mass Transfer, 109, 82–92.

[23] Kumar, R., Sood, S., Sheikholeslami, M., Shehzad, S.A., (2017): Nonlinear thermal radiation and cubic autocatalysis chemical reaction effects on the flow of stretched nanofluid under rotational oscillations, J. Colloid Interface Science, 505, 253–265.

[24] Koo, J., Kleinstreuer, C., (2005): Laminar nanofluid flow in microheat-sinks, Int. J. Heat Mass Transfer, 48, 2652–2661.

[25] Koo, J., Kleinstreuer, C., (2004): Viscous dissipation effects in micro tubes and micro channels, Int. J. Heat Mass Transfer, 47, 3159–3169.

[26] Batchlor, G. K., (1987): An introduction to fluid dynamics, Londan: Cambridge University Press, 158

[27] Rosseland, S., (1931): Astrophysik und atom-theoretischeGrundlagen, Springer-Verlag, Berlin.

[28] Liao, S. J., (2003): Beyond perturbation: Introduction to homotopy Analysis Method, Chapman and Hall/CRC Press, Boca Raton.

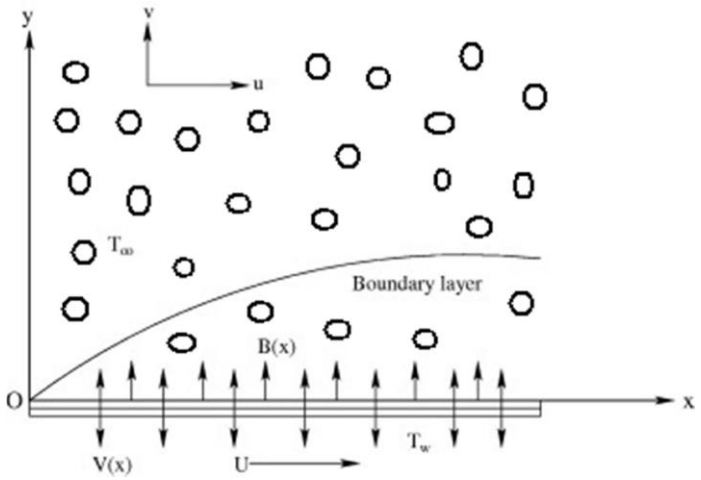


**Figure 1: Physical Sketch of Problem**

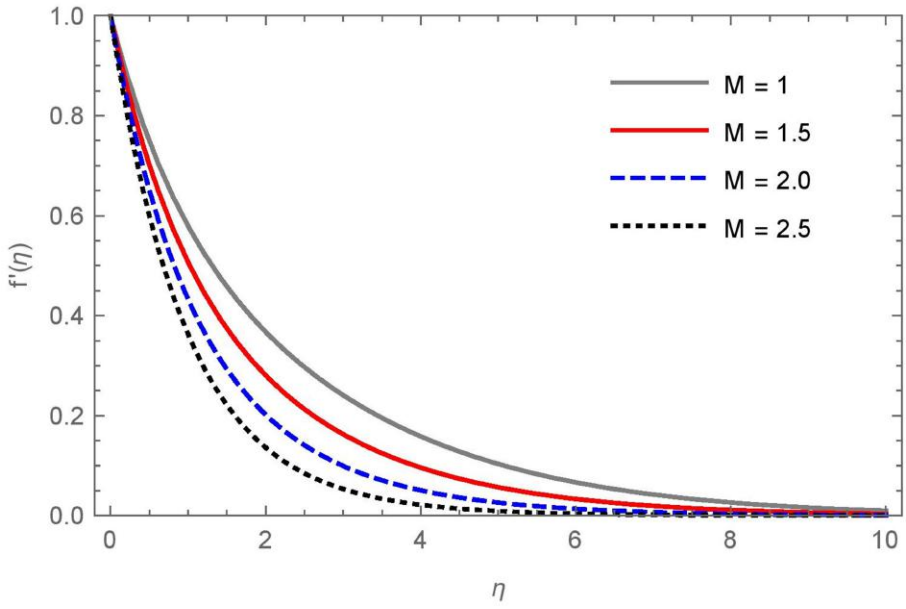


**Figure 2: Velocity Profile for Different value of *M***

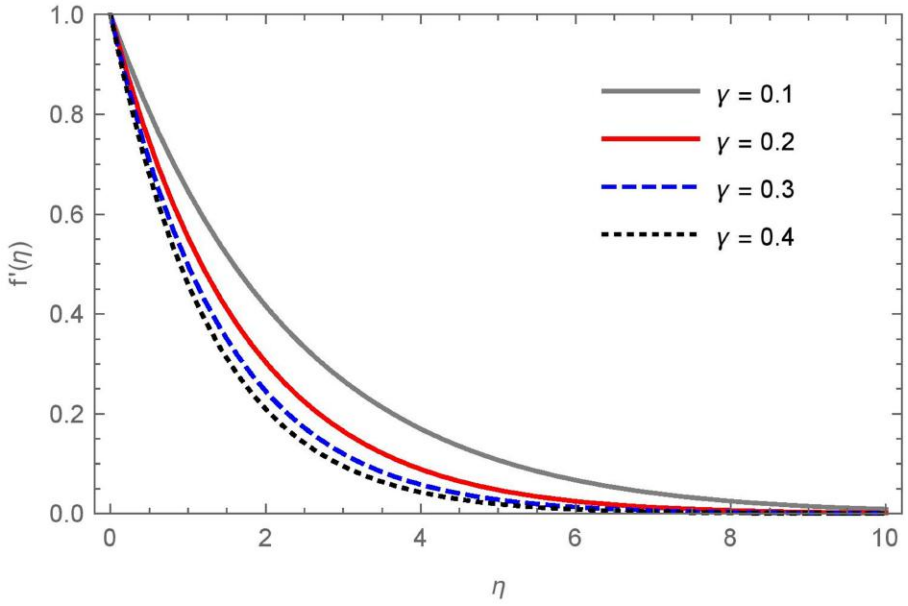


**Figure 3: Velocity Profile for Different value of $\gamma$**

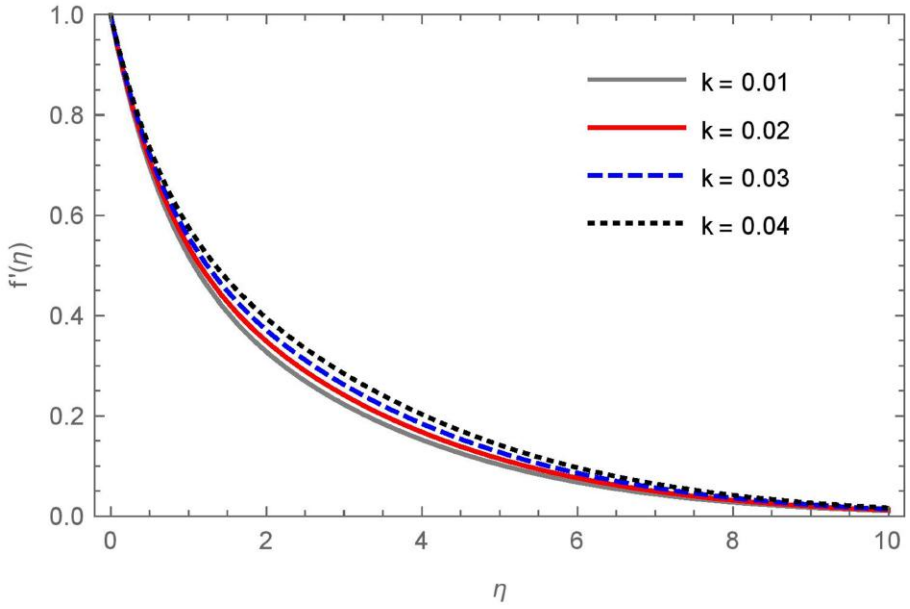


**Figure 4: Velocity Profile for Different value of $k$**

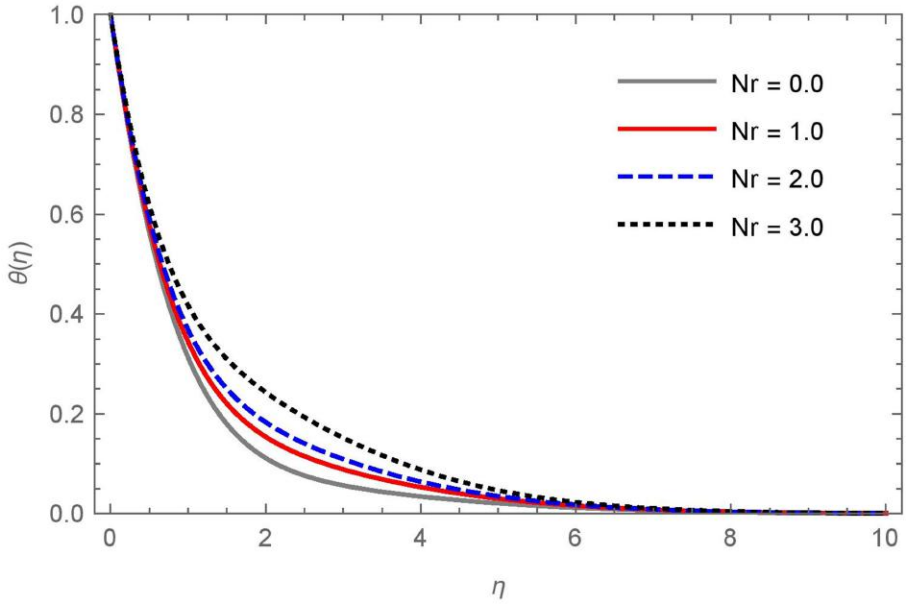


**Figure 5: Temperature Profile for Different value of $Nr$**

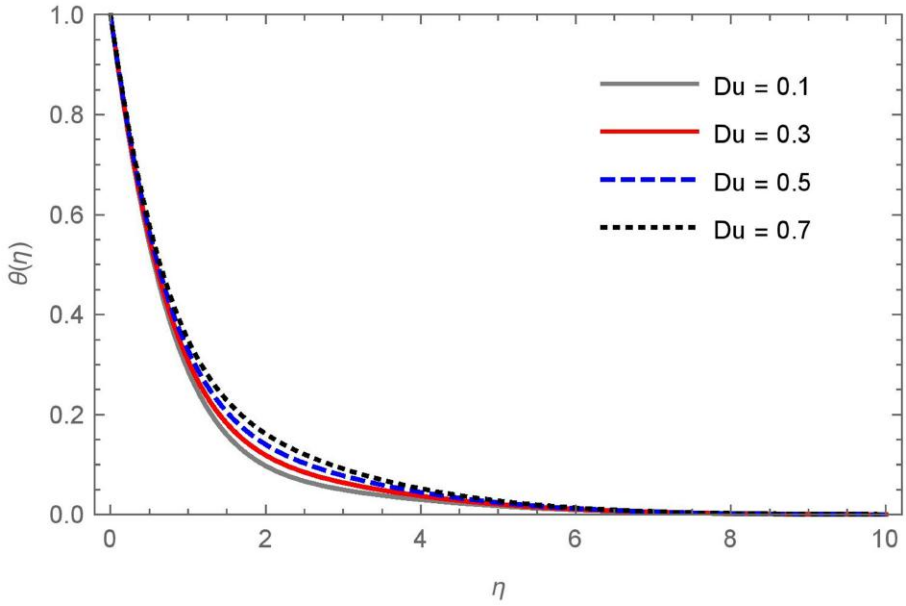


**Figure 6: Temperature Profile for Different value of $Du$**

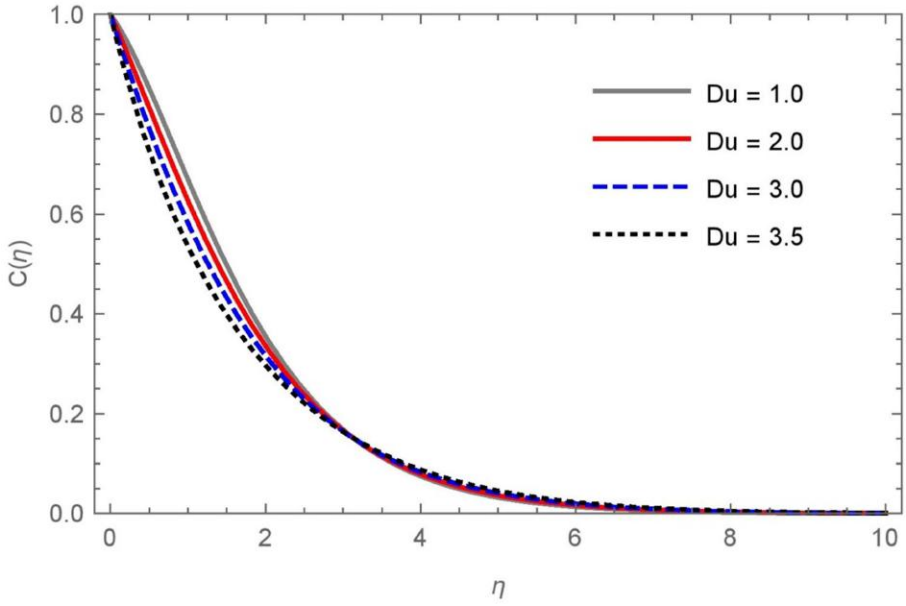


**Figure 7: Concentration Profile for Different value of $Du$**

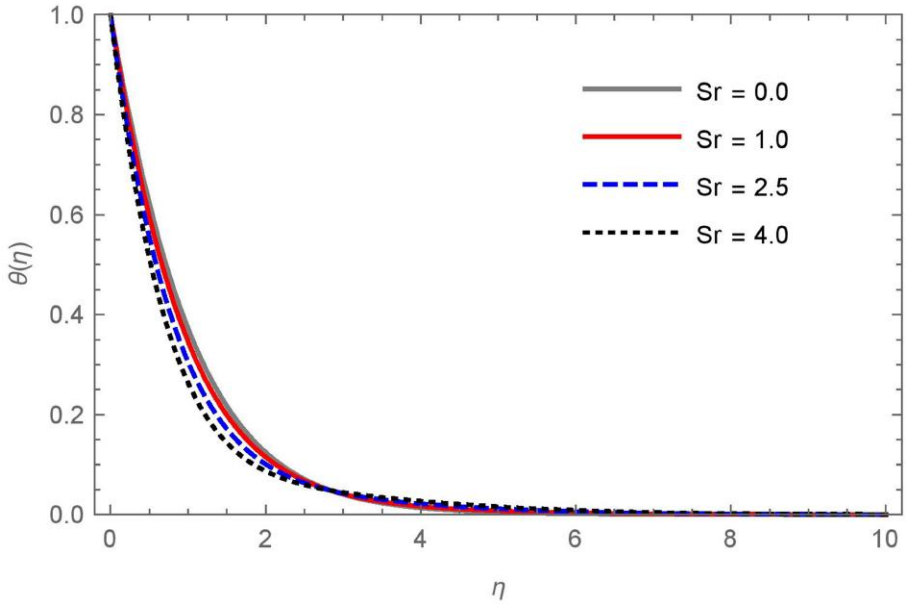


**Figure 8: Temperature Profile for Different value of $Sr$**

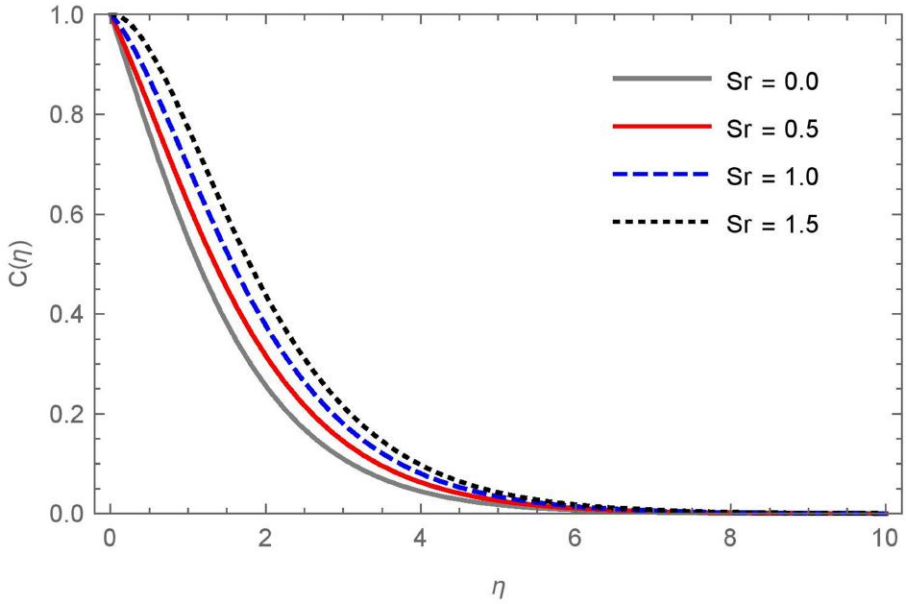


**Figure 9: Concentration Profile for Different value of *Sr***

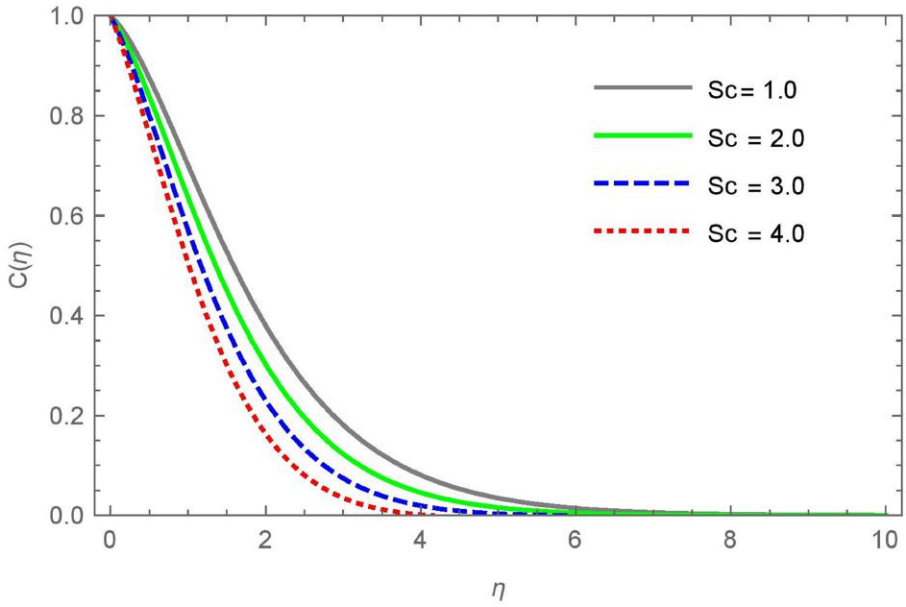


**Figure 10: Concentration Profile for Different value of *Sc***